Published in final edited form as:

Biochim Biophys Acta Mol Cell Biol Lipids. 2017 October ; 1862(10 Pt A): 1035–1043. doi:10.1016/j.bbalip.2017.07.001.

Hepatic ABCA1 deficiency is associated with delayed apolipoprotein B secretory trafficking and augmented VLDL triglyceride secretion

Mingxia Liu[1,#], **Soonkyu Chung**[1], **Gregory S. Shelness**[1], **John S. Parks**[1,2]

[1]Departments of Internal Medicine-Section on Molecular Medicine, Winston-Salem, NC, USA

[2]Biochemistry, Wake Forest School of Medicine, Winston-Salem, NC, USA

Abstract

ATP binding cassette transporter A1 (ABCA1) is a membrane transporter that facilitates nascent HDL formation. Tangier disease subjects with complete ABCA1 deficiency have <5% of normal levels of plasma HDL, elevated triglycerides (TGs), and defective vesicular trafficking in fibroblasts and macrophages. Hepatocyte-specific ABCA1 knockout mice (HSKO) have a similar lipid phenotype with 20% of normal plasma HDL levels and a two-fold elevation of plasma TGs due to hepatic overproduction of large, triglyceride-enriched VLDL. We hypothesized that enhanced VLDL TG secretion in the absence of hepatocyte ABCA1 is due to altered intracellular trafficking of apolipoprotein B (apoB), resulting in augmented TG addition to nascent VLDL. We found that trafficking of newly synthesized apoB through the secretory pathway was delayed in ABCA1-silenced rat hepatoma cells and HSKO primary hepatocytes, relative to controls. Endoglycosidase H treatment of cellular apoB revealed a likely delay in apoB trafficking in post-ER compartments. The reduced rate of protein trafficking was also observed for an adenoviral-expressed GPI-linked fluorescent fusion protein, but not albumin, suggesting a selective delay of secretory cargoes in the absence of hepatocyte ABCA1. Our results suggest an important role for hepatic ABCA1 in regulating secretory trafficking and modulating VLDL expansion during the TG accretion phase of hepatic lipoprotein particle assembly.

Supplementary keywords:

HDL deficiency; VLDL1; endoplasmic reticulum; Golgi apparatus; vesicular trafficking

1. Introduction

Hypertriglyceridemia is a key feature of metabolic syndrome, which has become a major health issue in the United States and globally (1). One of the primary causes of hypertriglyceridemia under conditions of insulin resistance is hepatic overproduction of large, TG-enriched VLDL particles (VLDL1) (2). VLDL maturation and secretion involves

[#]Correspondence to, Dr. Mingxia Liu, Department of Internal Medicine-Section on Molecular Medicine, Wake Forest School of Medicine, Medical Center Blvd., Winston-Salem, NC 27157, USA. Tel: 336-713-0325; Fax: 336-716-6279; mliu@wakehealth.edu.

The authors claim no conflict of interest.

at least two distinct steps (3). In the first step, apolipoprotein B (apoB) is cotranslationally translocated into the endoplasmic reticulum (ER) lumen where it undergoes initial lipidation catalyzed by microsomal TG transfer protein (MTP), forming pre-VLDL particles (4). During the second step, pre-VLDL particles fuse with bulk lipid droplets in the ER and/or post-ER compartments of the secretory pathway, forming mature VLDL particles destined for secretion. VLDL particles vary in size and composition (5) and can be separated into two main classes: large, buoyant VLDL1 particles (S_f > 100), which contain more TG, and smaller, more dense VLDL2 particles (S_f20–100) (6).

ABCA1 is a membrane bound transporter that facilitates free cholesterol and phospholipid efflux to lipid-free or -poor apoA-I, forming nascent HDL particles (7, 8). Complete absence of ABCA1 function causes Tangier disease (TD), a rare genetic disorder characterized by <5% normal HDL levels, a 50% decrease in plasma LDL, and a significant increase in plasma TG concentrations (9, 10). Chow-fed hepatocyte-specific ABCA1 knockout mice (HSKO) display a plasma lipid and lipoprotein phenotype similar to TD subjects, with 20% of normal plasma HDL levels, a 50% decrease in LDL concentrations, and a two-fold increase in plasma TG relative to wild type (WT) mice (11), suggesting that hepatic ABCA1 expression plays a major role in the TD plasma lipid/lipoprotein phenotype. Whereas the role of hepatocyte ABCA1 in HDL assembly and maintenance of plasma HDL concentrations is established, its role in regulating plasma TG concentrations is poorly understood. Previous studies demonstrated that silencing of ABCA1 in McArdle RH-7777 rat hepatoma cells (McA) increased the secretion of large TG-enriched VLDL1 particles (12). In addition, HSKO mice had increased secretion of VLDL1 particles and decreased post-heparin plasma lipase activity, both contributing to increased plasma TG levels (11). However, the cellular mechanism responsible for increased hepatic VLDL1 secretion in the absence of ABCA1 is unknown.

Schmitz *et al.* first demonstrated that TD is associated with defects in intracellular vesicle trafficking (13) and that fibroblasts and monocytes from TD patients displayed an enlarged Golgi morphology (14). In addition, vesicular trafficking of ceramide from Golgi to plasma membrane was shown to be decreased in TD fibroblasts (15). Subsequent studies demonstrated that secretion of fluorescent fusion proteins targeted to the plasma membrane was decreased in TD fibroblasts and macrophages (16); however, whether trafficking is defective in ABCA1 deficient hepatocytes has not been investigated.

In the present study, we tested the hypothesis that hepatocyte ABCA1 expression regulates the trafficking of vesicles containing VLDL cargo. We found that silencing ABCA1 in rat hepatoma cells delayed apoB trafficking in post-ER compartments coincident with increased secretion of VLDL1 particles. Primary hepatocytes from HSKO mice also showed slower trafficking of both apoB and an adenoviral-expressed fluorescent fusion protein; however, albumin secretion was not affected, suggesting a selective perturbation of secretory cargo trafficking to the plasma membrane in the absence of ABCA1. Reduced rates of intracellular trafficking may allow more time for VLDL particle expansion, resulting in secretion of larger TG-enriched VLDL1 particles in ABCA1 deficient hepatocytes.

2. Materials and Methods

2. 1. Materials and Reagents

Anti-human apoB100/48 antibody (Academy Bio-medical Inc., 20A-G1b), anti-albumin antibody (abcam, ab34807) and protein G Sepharose beads (Sigma-Aldrich, P3296) were used for immunoprecipitation. siRNA transfection experiments were performed using siRNA smartpool for ABCA1 (L-092371-02-0005), control siRNA (D-001810-0X) and Dharmafect 1 transfection reagent (T-2001–03) purchased from GE Healthcare. [^{35}S]-Methionine/Cysteine (Met/Cys) (NEG709A500UC) and [^{3}H]-oleic acid (NET289005MC) was purchased from Perkin Elmer. Endoglycosidase H (Endo H) (P0702L) and peptide N-glycosidase F2 (PNGase F) (P0704L) were purchased from New England Biolabs. Phosphatidylinositol-specific phospholipase C (PI-PLC, P-6466) was purchased from Life Technologies. Collagenase type I was purchased from Worthington (LS004197). Protease inhibitor cocktail was from Roche (11697498001). Cycloheximide (C7698), Methionine (M-2893) and Cysteine (C-8277) were from Sigma-Aldrich. Adenovirus titer kit was from Clontech (632250).

2. 2. Animals

ABCA1 HSKO mice were generated as described previously (17). ABCA1 HSKO mice were backcrossed into the C57Bl/6J background; wild type (ABCA1 flox/flox) and HSKO (ABCA1 flox/flox-Albumin Cre) mice for this study were generated from heterozygous matings. All animals were housed in a Wake Forest School of Medicine Animal Resources Program facility with a 12 h light/12 h dark cycle and fed *ad libitum* a commercial chow diet. All procedures were approved by the Institutional Animal Care and Use Committee of Wake Forest School of Medicine.

2. 3. Silencing ABCA1 in McA cells

McA cells (3×10^5 cells/well in 6-well collagen-coated plates) were cultured with DMEM containing 10% fetal bovine serum (FBS) throughout the experiment. Cells were transfected with either control or ABCA1 siRNA (50 nM) for 48 h as described previously (12), resulting in a >75% decrease in ABCA1 protein expression based on Western Blot analysis (12).

2. 4. Primary hepatocyte isolation

Primary hepatocytes were isolated as previously described (11). Briefly, mice were anesthetized with ketamine/xylazine. Livers were exposed and perfused via the portal vein with HBSS containing HEPES (10 mM) and EDTA (0.5 mM) until cleared of blood. Livers were then perfused with HBSS containing HEPES (10 mM), $CaCl_2$ (5 mM) and collagenase type I (0.3 mg/ml). Hepatocytes were released from dissected liver tissue into Williams′ media E and filtered through a 100 μm cell strainer, washed twice with the same media, collected by centrifugation (50 × g for 5 min), and seeded on collagen-coated dishes in Williams′ media E with penicillin/streptomycin, 10% FBS and 0.1 nM insulin. Cells were used for experiments within 24 h of isolation.

2. 5. VLDL TG secretion

McA cells were radiolabeled with [^{3}H]-oleic acid (1 μCi/ml) in DMEM containing penicillin/streptomycin, 10% FBS and 0.8 mM oleate for 16 h. Primary hepatocytes were incubated with [^{3}H]-oleic acid and 0.4 mM oleate for 6 h. After the radiolabeling period, media were harvested and lipids were extracted using the Bligh Dyer method (18). TLC was used to separate TG from other lipids in the extract. The TG band was isolated and quantified by scintillation counting. Cellular protein content was determined by Lowry assay and used to normalize radiolabeled TG values.

2. 6. Pulse-chase experiments

Both McA cells and primary hepatocytes were maintained at 37°C during the pulse-chase procedures. McA cells were pre-incubated with 0.8 mM oleate for 2 h before switching to Met/Cys-deficient media for 30 min. Cells were then radiolabeled with [^{35}S]-Met/Cys (100 μCi) for the indicated periods of time (10 or 15 min), followed by addition of Met/Cys complete media (DMEM with 10%FBS, 10 mM Met and 3mM Cys) at the end of pulse period to terminate radiolabeling. The radiolabeling medium was then removed, cells were washed, and fresh Met/Cys complete medium was added for the indicated chase time before cell lysates and media were collected in Triton X-100 lysis buffer (1% Triton X-100, 25 mM Tris-HCl, pH 7.5, 150 mM NaCl) containing protease inhibitor cocktail. Cells collected immediately following the pulse period represent the 0-min chase time point. Cell lysate and media samples were subjected to immunoprecipitation, as described below.

2. 7. Immunoprecipitation of apoB and albumin in hepatocyte cell lysates and medium

Cell lysate and media in lysis buffer were rotated with indicated antibodies overnight at 4°C. Protein G Sepharose beads were added and rotated for another 2 h before the beads were centrifuged, washed three times with lysis buffer, and then once with washing buffer (0.1% SDS, 10 mM Tris-HCl, pH 7.5, 2.5 mMEDTA). ApoB immunoprecipitates were denatured at 37°C for 30 min with NuPage® LDS sample buffer containing dithiothreitol (100 mM); albumin immunoprecipitates were denatured at 95°C for 5 min. Six and 8% SDS-PAGE were used to resolve apoB and albumin, respectively. Gels were heated and dried under vacuum and radiolabeled proteins were visualized using a phosphorimager (Fujifilm). Band intensities were quantified using Multi Gauge software (Fujifilm).

2. 8. Endo H and PNGase F treatment

Immunoprecipitated cellular apoB was reconstituted in denaturing buffer (0.5% SDS, 40 mM DTT) and treated with or without Endo H in the presence of protease inhibitors at 37°C for 1 h. To fully cleave all N-linked glycans, aliquots of apoB immunoprecipitates were treated with PNGase F in the presence of denaturing buffer, 10% NP40 and protease inhibitors, as recommended by the supplier.

2. 9. Adenovirus YFP-GPI expression

Adenovirus expressing a glycosylphosphatidylinositol-linked yellow fluorescence protein (YFP-GPI), generously provided by Drs. Ruth McPherson (University of Ottawa) (16) and Kai Simons (Max Planck Institute) (19), was amplified in HEK293 cells, and titrated using

an adenovirus titer kit. Viral particles, used at a multiplicity of infection of 100, were used to infect primary hepatocytes. Twenty-four h after infection, hepatocytes were cooled to 19.5°C for 2–4 h to block vesicular trafficking; during the last 30 min of the temperature block, cycloheximide (25 μg/ml) was added to inhibit protein synthesis. After the temperature block, cells were warmed to 32°C for 30 min and fixed with 4% paraformaldehyde for visualization under a fluorescence microscope (Olympus). In experiments using PI-PLC, after the temperature block, cells were warmed to 37°C for 30 min and then incubated at 19.5°C for 2 h with PI-PLC before media and cell lysates were collected and fluorescence intensity was measured using a FLUOstar microplate reader (BMG Labtech).

2. 10. Statistical Analysis

Data are presented as mean ± SEM. Two-tailed student′s *t* tests were used to compare means between groups. Two-way ANOVA were used to analyze results in Figure 2B and C. Statistical analyses were performed using GraphPad Prism. Differences at $p<0.05$ were considered statistically significant and indicated by * on plots.

3. Results

3. 1. Silencing of ABCA1 in McA hepatom a cells delays apoB trafficking

In ABCA1 siRNA-treated McA cells, secretion of [^{3}H]-oleic acid-radiolabeled VLDL TG significantly increased compared to control siRNA-treated cells (Figure 1A), as observed in previous studies (12). However, secretion of newly synthesized apoB was similar for control vs. ABCA1 siRNA treatment (Figure 1B), suggesting that increased TG secretion was mainly due to increased VLDL TG content, not VLDL particle number. As VLDL particle assembly and lipidation occur in the ER and Golgi, we investigated whether the increased VLDL-TG secretion observed with ABCA1 silencing was due to delayed VLDL particle trafficking, allowing more time for TG enrichment of nascent VLDL.

To assess the VLDL secretion kinetics, we monitored apoB secretion by pulse-chase analysis (Figure 2A). As apoB100 is more abundantly expressed in McA cells than apoB48 (Figure 1B), we focused our quantitative analysis on apoB100 secretion (Figure 2B), although similar trends were observed for apoB48. At the end of a 15 min radiolabel pulse (0 min chase), there was no apparent difference in cellular apoB100 abundance for control and ABCA1 siRNA-treated cells, indicating that ABCA1 depletion did not alter apoB synthesis in McA cells (Figure 2A; 0 min). After a 30 min chase, radiolabel apoB reached its maximum levels and apoB began to appear in media (Figure 2A; 30 min). We calculated the percentage of cellular (Figure 2B) and secreted apoB (Figure 2C) at 45, 60, 90 and 180 min by normalizing to 30 min chase cellular apoB100 levels and found a significant increase in cellular apoB100 in ABCA1 siRNA vs. control groups by two-way ANOVA, which was dominated by 60 and 90 min chase time points (Figure 2B). Because cellular apoB is regulated in co- and post-translational turnover pathways (20), higher cellular apoB in ABCA1 siRNA-treated cells could result from decreased apoB trafficking or degradation or a combination of both. We next assessed apoB100 degradation by calculating the percentage of radiolabel apoB100 remaining in cells and medium over time (Figure 2D) relative to cellular apoB100 levels at 30 min chase. ApoB degradation reached a maximum at the 60

min chase timepoint and was similar between control and ABCA1 siRNA-treated cells. These data suggest that delayed apoB trafficking, not decreased apoB degradation, resulted in increased cellular apoB100 levels in ABCA1 siRNA vs. control cells at the 60 and 90 min chase timepoints. We confirmed this finding in an independent experiment in which we pulse radiolabeled McA cells with [^{35}S]-Met/Cys for 10 min and chased for 60 min (Figure 2E & F) and observed an increase in cellular apoB100 and apoB48 in ABCA1 siRNA vs. control cells.

3. 2. ApoB trafficking is delayed in post-ER compartment in ABCA1-silenced McA cells

Pre-VLDL particle expansion with addition of bulk TG in the second step of VLDL particle assembly has been reported to occur in both ER and post-ER cellular compartments (21–25). To determine whether the observed delay in VLDL particle secretion in ABCA1-silenced McA cells occurred in the ER or post-ER cellular compartment, we examined sensitivity of apoB to Endo H, which cleaves only high mannose forms of glycoproteins, indicative of pre-Golgi localization. PNGase F was used as positive control for oligosaccharides cleavage, as it cleaves all forms of N-linked glycan chains. First, siRNA-treated McA cells were radiolabeled with [^{35}S]-Met/Cys for 4 h and cellular and media apoB were immunoprecipitated and incubated with Endo H, PNGase F, or no enzyme (control). Media apoB from both control and ABCA1 siRNA-treated McA cells showed resistance to Endo H but remained sensitive to PNGase F treatment (Figure 3A), suggesting that both apoB100 and apoB48 acquire Endo H resistance in post-ER compartments before secretion. In contrast, steady state cellular apoB remained sensitive to both Endo H and PNGase F (Figure 3B), indicating that the majority of cellular apoB at steady state is present in pre- and early Golgi compartments. Next, we studied apoB trafficking by pulse-chase analysis. siRNA treated-McA cells were pulse radiolabeled with [^{35}S]-Met/Cys for 10 min and chased for 60 min. Cellular apoB was then immunoprecipitated and incubated ± Endo H. After the 10 min pulse, there was no difference in radiolabeled apoB between control and ABCA1 siRNA-treated cells (data not shown), consistent with our previous experiment suggesting that ABCA1 did not affect apoB synthesis. After the 60 min chase period, ABCA1 siRNA-treated cells clearly contained more apoB (Figure 3C, lanes 4–6) compared to control siRNA-treated cells (lanes 1–3). These results were quantified in Figure 3D. With Endo H incubation, apoB100 displayed two distinct bands (Figure 3C; lanes 7–12); the upper band was an Endo H resistant form of apoB100, indicating its location in a post-ER compartment and the bottom band was the sensitive form of apoB100, suggesting ER and early Golgi localization. ApoB48 showed full sensitivity to Endo H treatment, likely due to longer residence time in the ER. Interestingly, we did not observe a difference in distribution of Endo H sensitive vs. resistant apoB100 between control and ABCA1 siRNA-treated cells (Figure 3C &E). These results suggest that delayed apoB trafficking occurs after apoB exits the ER, as differences in Endo H sensitivity would have been observed in control and ABCA1-silenced McA cells if the rate of trafficking out of the ER was delayed.

3. 3. ApoB trafficking is defective in primary hepatocytes lacking ABCA1

Next, we studied TG secretion and apoB trafficking in primary hepatocytes lacking ABCA1. Consistent with the results from ABCA1 siRNA-treated McA cells, hepatocytes from ABCA1 HSKO mice demonstrated increased TG secretion compared to wild type (WT)

mice (Figure 4A), in agreement with our previously published study (11). We also examined secretion of newly synthesized apoB from WT and ABCA1 HSKO mouse primary hepatocytes after a 10 min pulse radiolabel with [^{35}S]-Met/Cys and a 60 min chase with complete media. Primary mouse hepatocytes secreted mostly apoB48 compared to apoB100 (Figure 4B), due to higher apoB mRNA editing enzyme activity, relative to McA cells (26). Hepatocytes from ABCA1 HSKO mice displayed increased cellular apoB48 and apoB100 compared to hepatocytes from WT mice after the 60 min chase, suggesting a reduced rate of apoB trafficking (Figure 4B and quantification of apoB48 in Figure 4C). However, there was no apparent difference in apoB in medium between the two genotypes (Figure 4B & D). These data agree with the findings in ABCA1 siRNA-treated McA cells, further emphasizing that hepatic ABCA1 may play a critical role in regulating apoB trafficking kinetics.

3. 4. ABCA1 deficiency selectively affects secretory cargo trafficking kinetics

To determine whether the delay in apoB secretion from ABCA1 HSKO mouse hepatocytes was due to reduced trafficking of VLDL or a more generalized defect, we investigated an YFP-GPI fusion protein, used previously to investigate trafficking of vesicular cargo targeted to apical membrane lipid rafts in polarized and non-polarized cells (19). Primary hepatocytes were infected with adenovirus expressing YFP-GPI for 24 h and then, incubated at 19.5°C for 2 h to accumulate YFP-GPI in the Golgi, with cycloheximide added for the last 30 min to prevent further protein synthesis. Cells were warmed to 32°C and incubated for 20 min to allow movement of secretory proteins to the plasma membrane before they were fixed and imaged under a florescence microscope. At 19.5°C, fluorescent proteins accumulated in the Golgi in both WT and ABCA1 HSKO hepatocytes, as evidenced by hemi nuclear staining (Figure 5A). After 20 min of release, there was diffuse cytoplasmic localization of YFP-GPI in both WT and ABCA1 HSKO hepatocytes; however, WT hepatocytes displayed prominent plasma membrane staining whereas HSKO hepatocytes did not, suggesting that ABCA1 deficiency reduced YFP-GPI trafficking to the plasma membrane (Figure 5A). In another set of experiments, after the 19.5°C temperature block, cells were warmed to 37°C for 20 min and then treated with phosphatidylinositol specific-phospholipase C (PI-PLC) at 19.5°C to cleave YFP from its GPI anchor before medium and cell lysates were collected to measure fluorescence intensity. PI-PLC treatment showed an ~ 60% decrease in the ratio of membrane to cellular fluorescence intensity in ABCA1 HSKO hepatocytes (Figure 5B). These results suggest defective trafficking of both a GPI-linked protein and apoB in ABCA1 HSKO primary hepatocytes.

We next investigated the secretion kinetics of albumin, another major hepatic secretory protein, in WT and ABCA1 HSKO primary hepatocytes. Cells were pulse radiolabeled with [^{35}S]-Met/Cys for 15 min and chased for 30, 60 and 90 min (Figure 6A). At the end of the initial period (30 min chase), there was no significant difference in the amount of newly synthesized albumin in WT vs. ABCA1 HSKO hepatocytes, suggesting no difference in albumin synthesis between genotypes (Figure 6B). We also did not observe significant changes in cellular (Figure 6C) or media albumin (Figure 6D) in either of the 60 and 90 min chase samples from ABCA1 HSKO hepatocytes vs. WT cells, suggesting that albumin secretion kinetics are not altered in ABCA1-deficient hepatocytes. Combined with previous

data, this suggests a selective delay in protein secretion in the absence of hepatocyte ABCA1.

4. Discussion

Hepatocyte ABCA1 plays a key role in forming nascent HDL and maintaining the plasma HDL pool (17). ABCA1 also has a less well understood role in regulating hepatic VLDL secretion. Our previous studies found that ABCA1 deficiency leads to increased VLDL TG secretion in McA cells, primary hepatocytes, and livers from ABCA1 HSKO mice (11, 12) and a recent study by Bi et al (27) shows increased TG secretion from hepatocyte-like cells derived from TD subjects′ pluripotent stem cells. Here, we investigated the role of ABCA1 in apoB secretory trafficking in McA cells and primary hepatocytes and made several novel observations. First, we demonstrated reduced apoB trafficking in ABCA1-silenced McA cells and hepatocytes from ABCA1 HSKO mice, which was associated with increased VLDL TG secretion. These results suggest that the reduced rate of apoB trafficking may offer a greater opportunity for pre-VLDLs to fuse with TG-enriched lipid droplets in the secretory pathway, leading to TG-enriched VLDL particles during the second step of VLDL assembly. Second, we found that slowed apoB trafficking was not due to decreased rate of movement from ER to Golgi, based on onset of Endo H resistance, and may therefore be the result of altered trafficking within the Golgi. Finally, we show that ABCA1 deficiency resulted in delayed secretory trafficking of a GPI-linked protein, but not albumin, suggesting selectivity in the trafficking defect caused by ABCA1 deficiency.

ApoB is regulated by degradation pathways that occur in ER and post-ER compartments (20, 28, 29). Our data (Figure 2) showed a significant increase in cellular apoB and a trend towards decreased apoB secretion at the 60 and 90 min chase timepoints. Although this could be due to decreased apoB degradation in ABCA1 siRNA-treated cells, we did not detect any difference in the amount of secreted apoB at the 180 min chase timepoint when most radiolabel apoB had been secreted. Thus, our combined results support delayed apoB secretion in ABCA1 siRNA-silenced cells.

Abundant evidence supports a role for ABCA1 is cellular vesicular trafficking (13, 14, 16). Fibroblasts and monocytes from TD patients displayed enlarged Golgi morphology (14), with decreased ceramide trafficking from Golgi to plasma membrane in TD fibroblasts (15). Subsequent studies demonstrated that trafficking of fluorescent fusion proteins YFP-GPI and YFP-VSVG, which are both targeted to the plasma membrane, was decreased in TD fibroblasts and macrophages (16). Yamuchi et al (30) also reported that ABCA1 facilitates retrograde sterol movement from the plasma membrane to the ER. Our results in McA cells and primary hepatocytes, along with these data (13–16), suggest that ABCA1 plays a critical role in modulating secretory protein and lipid trafficking. However, hepatocyte ABCA1 deficiency did not seem to slow albumin secretion kinetics, suggesting selectivity in secretory traffic defect caused by absence of ABCA1. This is also consistent with data showing that albumin and apoB do not occupy the same vesicle populations emanating from the ER (31). ABCA1 is located in the plasma membrane and in early endosomal and lysosomal cellular compartments (32, 33). Lysosomal hydrolysis mobilizes lipid droplet-associated cholesterol for ABCA1-dependent efflux under cholesterol loading condition

(34). We recently demonstrated that trafficking of LDL-derived lysosomal cholesterol to the plasma membrane is reduced in HSKO vs. control hepatocytes (35), suggesting ABCA1 may shuttle between lysosomes and the plasma membrane to facilitate cellular cholesterol efflux. ABCA1 may have similar function to shuttle lysosomal lipid droplet-associated cholesterol into TG-rich VLDL particles in the secretory pathway. Although we have no evidence to support a direct interaction between ABCA1 and apoB in hepatocytes (data not shown), whether ABCA1 associates with VLDL particles in the secretory pathway remains unknown and merits further investigation.

As an N-linked glycoprotein, apoB undergoes glycan modifications in the early Golgi, resulting in acquisition of Endo H resistance. Our results showed that the ratio of Endo H sensitive and resistant forms of apoB100 were unaffected by ABCA1 deficiency, suggesting that the observed reduced secretory rate results from perturbed post-ER apoB trafficking. Although controversial, considerable evidence suggests that the second step of VLDL assembly, involving addition of bulk lipid, occurs in the Golgi compartment (21–25). Hence, delayed transit within the Golgi could account for the enhanced apoB lipidation and VLDL1 production observed in the current studies.

ABCA1 is widely acknowledged to function as a membrane transporter that effluxes phospholipid and free cholesterol to lipid-free apoA-I, forming nascent particles (8). We previously reported that hepatocyte ABCA1 activity accounted for most of the plasma HDL pool (17, 36), suggesting that ABCA1 in this tissue is critical in maintaining plasma cholesterol homeostasis. In addition, studies using primary hepatocytes from ABCA1 total knockout mice suggested that nascent HDL formation might compete with VLDL particle secretion for available cellular cholesterol (37). Hence, in the absence of hepatocyte ABCA1, cholesterol that is not assembled into nascent HDL particles is available for VLDL secretion, providing a potential mechanism for enhanced VLDL assembly with ABCA1 deficiency. However, liver cholesterol levels in ABCA1 HSKO mice or cellular cholesterol content in ABCA1-silenced McA cells are not elevated compared to their respective controls (11, 12), suggesting alternative mechanisms for enhanced VLDL assembly in the absence of ABCA1.

We previously observed decreased PI3 kinase activation in ABCA1-silenced McA cells and hepatocytes lacking ABCA1, which was associated with increased VLDL secretion (11, 12). Activation of PI3 kinases by insulin inhibits both VLDL apoB and TG secretion (38, 39), in a process that involves post-ER presecretory proteolysis (40). Subsequent evidence suggests that sortilin (41–43), MTP and apo C-III (44, 45) are mediators of insulin-regulated apoB secretion. It is tempting to speculate that ABCA1 may modulate VLDL assembly via regulating PI3 kinase signaling. However, our evidence suggests that hepatocyte ABCA1 deficiency and insulin resistance occur by different mechanisms, despite the fact that both lead to diminished PI3 kinase activation and increased VLDL1 secretion (11). First, insulin resistance results in decreased apoB degradation and increased secretion, whereas hepatic ABCA1 deficiency slows apoB secretion, but does not appear to decrease its degradation. Further, insulin resistance is associated with reduced *sortilin* and increased *apoC-III* expression (44, 46), whereas ABCA1 deficiency has no such effect (data not shown). In addition, our previous evidence shows that ABCA1 HSKO and WT mice have similar

hepatic MTP protein expression (11). Thus, the mechanism by which ABCA1 regulates VLDL secretion is likely distinct from that of the canonical insulin signaling pathway.

VLDL assembly and particle expansion requires phospholipids on the particle monolayer surface and phospholipid transfer protein facilitates this step of VLDL maturation (47, 48). We observed a significant reduction of *pltp* gene expression in ABCA1 HSKO vs. WT hepatocytes (data not shown), which does not support a role of PLTP in enhanced VLDL assembly in ABCA1 HSKO hepatocytes. Recent evidence shows that induced-pluripotent stem cell-derived hepatocyte-like cells from TD patients have abrogated HDL biogenesis and enhanced triglyceride secretion, similar to ABCA1 HSKO hepatocytes, and elevated gene expression of angptl3 (27), which is a potent regulator of plasma TG clearance and VLDL TG secretion (49–51). Agreeing with this data, we also saw a significant increase in *angptl3* gene expression in ABCA1 HSKO vs. WT hepatocytes (data not shown). Since angptl3 is a target of insulin signaling (52, 53), whether this change in its expression is simply a result of decreased insulin signaling in ABCA1 deficient hepatocytes or it contributes to enhanced VLDL assembly remains unknown and requires further investigation.

In summary, we have provided evidence for a novel role of hepatic ABCA1 in modulating vesicular trafficking, which may regulate VLDL assembly. These data help to rationalize the basis for lipid phenotypes associated with ABCA1 deficiency in mice and in humans with Tangier disease. Clarifying the mechanisms by which ABCA1 modulates VLDL and TG secretion may also reveal important regulatory nodes in the VLDL assembly pathway with relevance to hepatic lipid dysregulation associated with metabolic diseases, including fatty liver disease and plasma hypertriglyceridemia.

Acknowledgments

We gratefully acknowledge Karen Klein (Biomedical Research Services and Administration, Wake Forest School of Medicine) for editing the manuscript and Drs. Ruth McPherson (University of Ottawa) and Kai Simons (Max Planck Institute) for supplying adenovirus YFP-GPI. This project was supported by National Institutes of Health Grants (P01HL49373 to [JSP & GSS] and R01HL119962 to JSP) and American Heart Association Pre-doctoral Fellowship (12PRE12040309 to ML) and RJR-Leon Golberg Post-doctoral Fellowship to ML. This article was prepared while Gregory S. Shelness was employed by Wake Forest School of Medicine. The opinions expressed in this article are the authors′ own and do not reflect the view of the National Institutes of Health, the Department of Health and Human Services, or the United States government.

Abbreviations:

ABCA1	ATP binding cassette transporter A1
TG	triglyceride
HSKO	hepatocyte-specific knockout
apoB	apolipoprotein B
McA	rat hepatoma McA RH7777 cells
Endo H	endoglycosidase H

PNGase F	peptide N-glycosidase F2
MTP	microsomal triglyceride transfer protein
TD	Tangier disease
YFP-GPI	yellow fluorescence protein-glycosylphosphatidylinositol
PI-PLC	phosphatidylinositol-specific phospholipase C
apoC-III	apolipoprotein C-III
PC	phosphatidylcholine
PE	phosphatidylethanolamine

References

1. O′Neill S, and O′Driscoll L. 2015 Metabolic syndrome: a closer look at the growing epidemic and its associated pathologies. Obes Rev 16: 1–12.
2. Taskinen MR 1995 Insulin resistance and lipoprotein metabolism. Curr Opin Lipidol 6: 153–160. [PubMed: 7648004]
3. Olofsson SO, Stillemark-Billton P, and Asp L. 2000 Intracellular assembly of VLDL: two major steps in separate cell compartments. Trends CardiovascMed 10: 338–345.
4. Davidson NO, and Shelness GS. 2000 APOLIPOPROTEIN B: mRNA editing, lipoprotein assembly, and presecretory degradation. Annu Rev Nutr 20: 169–193. [PubMed: 10940331]
5. Lossow WJ, Lindgren FT, Murchio JC, Stevens GR, and Jensen LC. 1969 Particle size and protein content of six fractions of the Sf 20 plasma lipoproteins isolated by density gradient centrifugation. J Lipid Res 10: 68–76. [PubMed: 5764118]
6. Wang Y, Tran K, and Yao Z. 1999 The activity of microsomal triglyceride transfer protein is essential for accumulation of triglyceride within microsomes in McA-RH7777 cells. A unified model for the assembly of very low density lipoproteins. J Biol Chem 274: 27793–27800. [PubMed: 10488124]
7. Yokoyama S 2006 Assembly of high-density lipoprotein. Arterioscler Thromb Vasc Biol 26: 20–27. [PubMed: 16284193]
8. Lee JY, and Parks JS. 2005 ATP-binding cassette transporter AI and its role in HDL formation. Curr Opin Lipidol 16: 19–25. [PubMed: 15650559]
9. Kolovou G, Daskalova D, Anagnostopoulou K, Hoursalas I, Voudris V, Mikhailidis DP, and Cokkinos DV. 2003 Postprandial hypertriglyceridaemia in patients with Tangier disease. J Clin Pathol 56: 937–941. [PubMed: 14645354]
10. Fredrickson DS, Altrocchi PH, Avioli LV, Goodman DWS, and Goodman HC. 1961 Tangier disease: combined clinical staff conference at the national institutes of health. Annals of internal medicine 55.
11. Chung S, Timmins JM, Duong M, Degirolamo C, Rong S, Sawyer JK, Singaraja RR, Hayden MR, Maeda N, Rudel LL, Shelness GS, and Parks JS. 2010 Targeted deletion of hepatocyte ABCA1 leads to very low density lipoprotein triglyceride overproduction and low density lipoprotein hypercatabolism. Journal of Biological Chemistry 285: 12197–12209. [PubMed: 20178985]
12. Chung S, Gebre AK, Seo J, Shelness GS, and Parks JS. 2010 A novel role for ABCA1-generated large pre-beta migrating nascent HDL in the regulation of hepatic VLDL triglyceride secretion. Journal of Lipid Research 51: 729–742. [PubMed: 20215580]
13. Schmitz G, Assmann G, Robenek H, and Brennhausen B. 1985 Tangier disease: a disorder of intracellular membrane traffic. Proc Natl Acad Sci U S A 82: 6305–6309. [PubMed: 2994070]
14. Robenek H, and Schmitz G. 1991 Abnormal processing of Golgi elements and lysosomes in Tangier disease. Arterioscler Thromb 11: 1007–1020. [PubMed: 2065025]

15. Orso E, Broccardo C, Kaminski WE, Bottcher A, Liebisch G, Drobnik W, Gotz A, Chambenoit O, Diederich W, Langmann T, Spruss T, Luciani MF, Rothe G, Lackner KJ, Chimini G, and Schmitz G. 2000 Transport of lipids from golgi to plasma membrane is defective in tangier disease patients and Abc1-deficient mice. Nat Genet 24: 192–196. [PubMed: 10655069]
16. Zha X, Gauthier A, Genest J, and McPherson R. 2003 Secretory vesicular transport from the Golgi is altered during ATP-binding cassette protein A1 (ABCA1)-mediated cholesterol efflux. J Biol Chem 278:10002–10005. [PubMed: 12551894]
17. Timmins JM, Lee JY, Boudyguina E, Kluckman KD, Brunham LR, Mulya A, Gebre AK, Coutinho JM, Colvin PL, Smith TL, Hayden MR, Maeda N, and Parks JS. 2005 Targeted inactivation of hepatic Abca1 causes profound hypoalphalipoproteinemia and kidney hypercatabolism of apoA-I. J Clin Invest 115: 1333–1342. [PubMed: 15841208]
18. Bligh EG, and Dyer WJ. 1959 A rapid method of total lipid extraction and purification. Can J Biochem Physiol 37: 911–917. [PubMed: 13671378]
19. Keller P, Toomre D, Diaz E, White J, and Simons K. 2001 Multicolour imaging of post-Golgi sorting and trafficking in live cells. Nat Cell Biol 3: 140–149. [PubMed: 11175746]
20. Rutledge AC, Su Q, and Adeli K. Apolipoprotein B100 biogenesis: a complex array of intracellular mechanisms regulating folding, stability, and lipoprotein assembly. Biochem Cell Biol 88: 251–267. [PubMed: 20453928]
21. Gusarova V, Brodsky JL, and Fisher EA. 2003 Apolipoprotein B100 exit from the endoplasmic reticulum (ER) is COPII-dependent, and its lipidation to very low density lipoprotein occurs post-ER. J Biol Chem 278: 48051–48058. [PubMed: 12960170]
22. Tran K, Thorne-Tjomsland G, DeLong CJ, Cui Z, Shan J, Burton L, Jamieson JC, and Yao Z. 2002 Intracellular assembly of very low density lipoproteins containing apolipoprotein B100 in rat hepatoma McA-RH7777 cells. J Biol Chem 277: 31187–31200. [PubMed: 12065576]
23. Yamaguchi J, Gamble MV, Conlon D, Liang JS, and Ginsberg HN. 2003 The conversion of apoB100 low density lipoprotein/high density lipoprotein particles to apoB100 very low density lipoproteins in response to oleic acid occurs in the endoplasmic reticulum and not in the Golgi in McA RH7777 cells. J Biol Chem 278: 42643–42651. [PubMed: 12917397]
24. Swift LL 1995 Assembly of very low density lipoproteins in rat liver: a study of nascent particles recovered from the rough endoplasmic reticulum. J Lipid Res 36: 395–406. [PubMed: 7775852]
25. Swift LL, Valyi-Nagy K, Rowland C, and Harris C. 2001 Assembly of very low density lipoproteins in mouse liver: evidence of heterogeneity of particle density in the Golgi apparatus. J Lipid Res 42: 218–224. [PubMed: 11181751]
26. Wang S, Chen Z, Lam V, Han J, Hassler J, Finck BN, Davidson NO, and Kaufman RJ. 2012 IRE1alpha-XBP1s Induces PDI Expression to Increase MTP Activity for Hepatic VLDL Assembly and Lipid Homeostasis. Cell Metab 16: 473–486. [PubMed: 23040069]
27. Bi X, Pashos EE, Cuchel M, Lyssenko NN, Hernandez M, Picataggi A, McParland J, Yang W, Liu Y, Yan R, Yu C, DerOhannessian SL, Phillips MC, Morrisey EE, Duncan SA, and Rader DJ. 2017 ATP-Binding Cassette Transporter A1 Deficiency in Human Induced Pluripotent Stem Cell-Derived Hepatocytes Abrogates HDL Biogenesis and Enhances Triglyceride Secretion. EBioMedicine 18: 139–145. [PubMed: 28330813]
28. Liu M, Chung S, Shelness GS, and Parks JS. 2012 Hepatic ABCA1 and VLDL triglyceride production. Biochim Biophys Acta 1821: 770–777. [PubMed: 22001232]
29. Twisk J, Gillian-Daniel DL, Tebon A, Wang L, Barrett PH, and Attie AD. 2000 The role of the LDL receptor in apolipoprotein B secretion. J Clin Invest 105: 521–532. [PubMed: 10683382]
30. Yamauchi Y, Iwamoto N, Rogers MA, Abe-Dohmae S, Fujimoto T, Chang CC, Ishigami M, Kishimoto T, Kobayashi T, Ueda K, Furukawa K, Chang TY, and Yokoyama S. 2015 Deficiency in the Lipid Exporter ABCA1 Impairs Retrograde Sterol Movement and Disrupts Sterol Sensing at the Endoplasmic Reticulum. J Biol Chem 290: 23464–23477. [PubMed: 26198636]
31. Tiwari S, and Siddiqi SA. 2012 Intracellular trafficking and secretion of VLDL. Arterioscler Thromb Vasc Biol 32: 1079–1086. [PubMed: 22517366]
32. Neufeld EB, Remaley AT, Demosky SJ, Stonik JA, Cooney AM, Comly M, Dwyer NK, Zhang M, Blanchette-Mackie J, Santamarina-Fojo S, and Brewer HB Jr. 2001 Cellular localization and

trafficking of the human ABCA1 transporter. J Biol Chem 276: 27584–27590. [PubMed: 11349133]

33. Haidar B, Kiss RS, Sarov-Blat L, Brunet R, Harder C, McPherson R, and Marcel YL. 2006 Cathepsin D, a lysosomal protease, regulates ABCA1-mediated lipid efflux. J Biol Chem 281: 39971–39981. [PubMed: 17032648]
34. Ouimet M, Franklin V, Mak E, Liao X, Tabas I, and Marcel YL. 2011 Autophagy regulates cholesterol efflux from macrophage foam cells via lysosomal acid lipase. Cell Metab 13: 655–667. [PubMed: 21641547]
35. Key C-CC, Liu M, Kurtz CL, Chung S, Boudyguina E, Dinh TA, Bashore A, Phelan PE, Freedman BI, Osborne TF, Zhu X, Ma L, Sethupathy P, Biddinger SB, and Parks JS. 2017 Hepatocyte ABCA1 Deletion Impairs Liver Insulin Signaling and Lipogenesis. Cell Reports 19: 2116–2129. [PubMed: 28591582]
36. Brunham LR, Kruit JK, Iqbal J, Fievet C, Timmins JM, Pape TD, Coburn BA, Bissada N, Staels B, Groen AK, Hussain MM, Parks JS, Kuipers F, and Hayden MR. 2006 Intestinal ABCA1 directly contributes to HDL biogenesis in vivo. J Clin Invest 116: 1052–1062. [PubMed: 16543947]
37. Sahoo D, Trischuk TC, Chan T, Drover VA, Ho S, Chimini G, Agellon LB, Agnihotri R, Francis GA, and Lehner R. 2004 ABCA1-dependent lipid efflux to apolipoprotein A-I mediates HDL particle formation and decreases VLDL secretion from murine hepatocytes. J Lipid Res 45: 1122–1131. [PubMed: 14993246]
38. Brown AM, and Gibbons GF. 2001 Insulin inhibits the maturation phase of VLDL assembly via a phosphoinositide 3-kinase-mediated event. Arterioscler Thromb Vasc Biol 21: 1656–1661. [PubMed: 11597941]
39. Chirieac DV, Davidson NO, Sparks CE, and Sparks JD. 2006 PI3-kinase activity modulates apo B available for hepatic VLDL production in apobec-1−/− mice. Am J Physiol Gastrointest Liver Physiol 291: G382–388. [PubMed: 16798720]
40. Phung TL, Roncone A, Jensen KL, Sparks CE, and Sparks JD. 1997 Phosphoinositide 3-kinase activity is necessary for insulin-dependent inhibition of apolipoprotein B secretion by rat hepatocytes and localizes to the endoplasmic reticulum. J Biol Chem 272: 30693–30702. [PubMed: 9388205]
41. Chamberlain JM, O′Dell C, Sparks CE, and Sparks JD. 2012 Insulin suppression of apolipoprotein B in McArdle RH7777 cells involves increased sortilin 1 interaction and lysosomal targeting. Biochem Biophys Res Commun 430: 66–71. [PubMed: 23159624]
42. Musunuru K, Strong A, Frank-Kamenetsky M, Lee NE, Ahfeldt T, Sachs KV, Li X, Li H, Kuperwasser N, Ruda VM, Pirruccello JP, Muchmore B, Prokunina-Olsson L, Hall JL, Schadt EE, Morales CR, Lund-Katz S, Phillips MC, Wong J, Cantley W, Racie T, Ejebe KG, Orho-Melander M, Melander O, Koteliansky V, Fitzgerald K, Krauss RM, Cowan CA, Kathiresan S, and Rader DJ. 2010 From noncoding variant to phenotype via SORT1 at the 1p13 cholesterol locus. Nature 466: 714–719. [PubMed: 20686566]
43. Strong A, Ding Q, Edmondson AC, Millar JS, Sachs KV, Li X, Kumaravel A, Wang MY, Ai D, Guo L, Alexander ET, Nguyen D, Lund-Katz S, Phillips MC, Morales CR, Tall AR, Kathiresan S, Fisher EA, Musunuru K, and Rader DJ. 2012 Hepatic sortilin regulates both apolipoprotein B secretion and LDL catabolism. J Clin Invest 122: 2807–2816. [PubMed: 22751103]
44. Altomonte J, Cong L, Harbaran S, Richter A, Xu J, Meseck M, and Dong HH. 2004 Foxo1 mediates insulin action on apoC-III and triglyceride metabolism. J Clin Invest 114: 1493–1503. [PubMed: 15546000]
45. Kamagate A, Qu S, Perdomo G, Su D, Kim DH, Slusher S, Meseck M, and Dong HH. 2008 FoxOl mediates insulin-dependent regulation of hepatic VLDL production in mice. J Clin Invest 118: 2347–2364. [PubMed: 18497885]
46. Ai D, Baez JM, Jiang H, Conlon DM, Hernandez-Ono A, Frank-Kamenetsky M, Milstein S, Fitzgerald K, Murphy AJ, Woo CW, Strong A, Ginsberg HN, Tabas I, Rader DJ, and Tall AR. 2012 Activation of ER stress and mTORC1 suppresses hepatic sortilin-1 levels in obese mice. J Clin Invest 122: 1677–1687. [PubMed: 22466652]
47. Okazaki H, Goldstein JL, Brown MS, and Liang G. 2010 LXR-SREBP-1c-phospholipid transfer protein axis controls very low density lipoprotein (VLDL) particle size. J Biol Chem 285: 6801–6810. [PubMed: 20037162]

48. Yazdanyar A, and Jiang XC. 2012 Liver phospholipid transfer protein (PLTP) expression with a PLTP-null background promotes very low-density lipoprotein production in mice. Hepatology 56: 576–584. [PubMed: 22367708]

49. Wang Y, Gusarova V, Banfi S, Gromada J, Cohen JC, and Hobbs HH. 2015 Inactivation of ANGPTL3 reduces hepatic VLDL-triglyceride secretion. J Lipid Res 56: 1296–1307. [PubMed: 25954050]

50. Romeo S, Yin W, Kozlitina J, Pennacchio LA, Boerwinkle E, Hobbs HH, and Cohen JC. 2009 Rare loss-of-function mutations in ANGPTL family members contribute to plasma triglyceride levels in humans. J Clin Invest 119: 70–79. [PubMed: 19075393]

51. Robciuc MR, Maranghi M, Lahikainen A, Rader D, Bensadoun A, Oorni K, Metso J, Minicocci I, Ciociola E, Ceci F, Montali A, Arca M, Ehnholm C, and Jauhiainen M. 2013 Angptl3 deficiency is associated with increased insulin sensitivity, lipoprotein lipase activity, and decreased serum free fatty acids. Arterioscler Thromb Vasc Biol 33: 1706–1713. [PubMed: 23661675]

52. Nidhina Haridas PA, Soronen J, Sadevirta S, Mysore R, Quagliarini F, Pasternack A, Metso J,Perttila J, Leivonen M, Smas CM, Fischer-Posovszky P, Wabitsch M, Ehnholm C, Ritvos O, Jauhiainen M, Olkkonen VM, and Yki-Jarvinen H. 2015 Regulation of Angiopoietin-Like Proteins (ANGPTLs) 3 and 8 by Insulin. J Clin EndocrinolMetab 100: E1299–1307.

53. Shimamura M, Matsuda M, Ando Y, Koishi R, Yasumo H, Furukawa H, and Shimomura I. 2004 Leptin and insulin down-regulate angiopoietin-like protein 3, a plasma triglyceride-increasing factor. Biochem Biophys Res Commun 322: 1080–1085. [PubMed: 15336575]

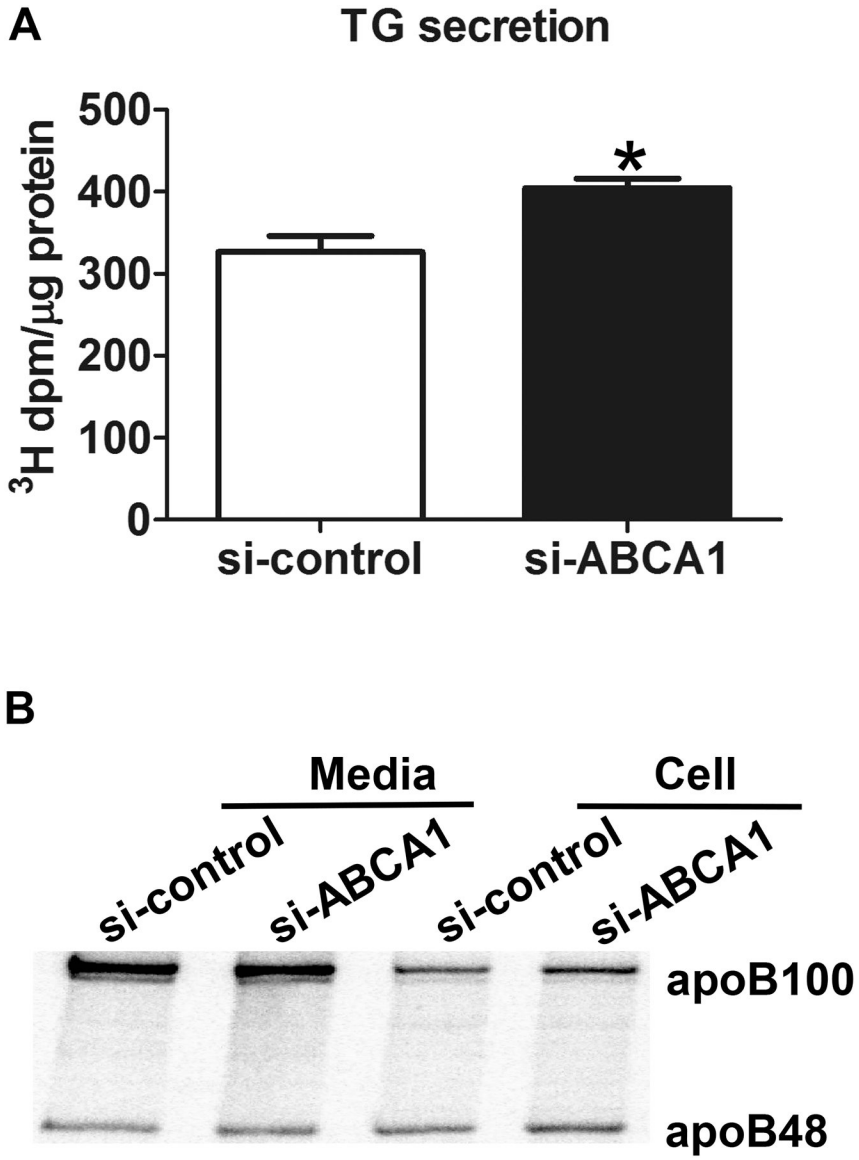

Figure 1. ABCA1 siRNA-treated McA cells display increased VLDL TG secretion without increased apoB secretion

McA cells were transfected with either control or ABCA1 siRNA for 48 h. (**A**) Cells were radiolabeled with [^{3}H]-oleic acid in the presence of unlabeled oleate for 16 h and media [^{3}H]-TG was quantified after lipid extraction and TLC fractionation; radiolabeled TG values were normalized to cellular protein content. (**B**) Cells were radiolabeled with [^{35}S]-Met/Cys for 4 h. ApoB immunoprecipitated from cells and media was fractionated by SDS-PAGE and visualized using a phosphorimager.

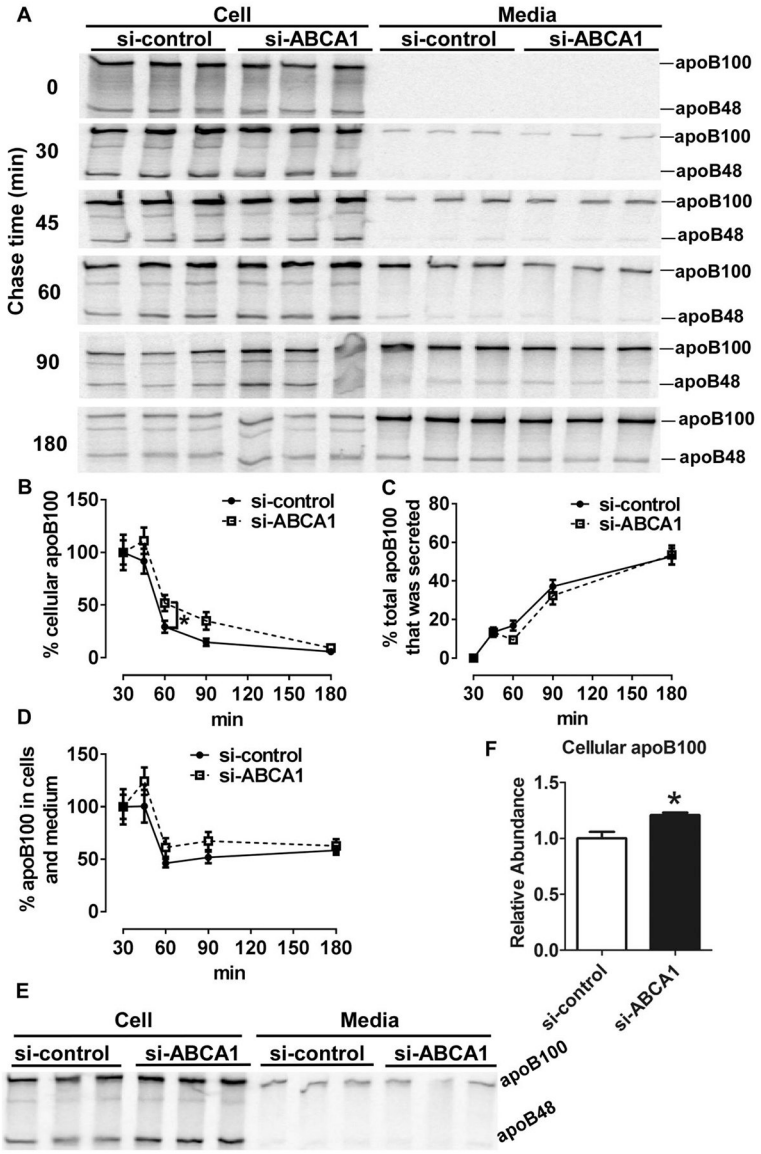

Figure 2. Silencing ABCA1 in McA cells causes a delay in apoB secretion

(**A**) McA cells were transfected with control or ABCA1 siRNA for 48 h, pulse radiolabeled with [^{35}S]-Met/Cys for 15 min, and chased with Met/Cys complete media for 0, 30, 45, 60, 90 and 180 min. Cellular and secreted [^{35}S]-apoB were visualized by phosphorimaging after apoB immunoprecipitation and SDS-PAGE separation. ApoB100 in panel A was quantified and its cellular (**B**), secreted level (**C**) and total radiolabel in cells and medium (**D**) were plotted as the percentage of cellular apoB present at the 30 min chase time point. (**E**) McA cells were transfected with control or ABCA1 siRNA for 48 h, pulse radiolabeled with [^{35}S]-Met/Cys for 10 min, and chased for 60 min. Cellular and secreted [^{35}S]-apoB were visualized using a phosphorimager. (**F**) ApoB100 abundance in panel E was quantified and plotted relative to control cells.

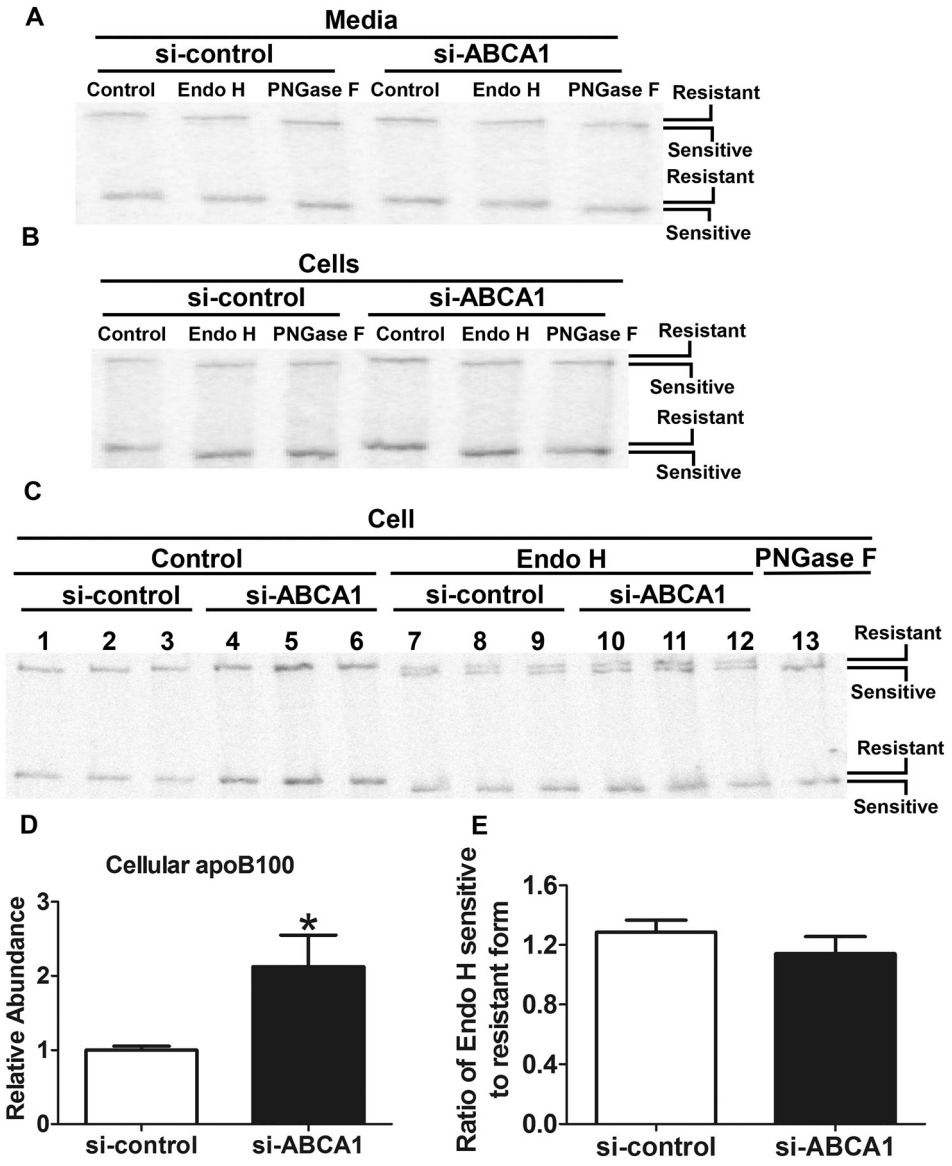

Figure 3. ApoB Endo H sensitivity is unaffected by ABCA1 deficiency

siRNA-treated McA cells were radiolabeled with [^{35}S]-Met/Cys for 4 h and cells (**A**) and media (**B**) were collected. ApoB was immunoprecipitated and aliquots were incubated with or without Endo H or PNGase F, separated by SDS-PAGE, and visualized with a phosphorimager. The gel mobility of glycosidase-sensitive and -resistant forms of apoB100 and apoB48 are indicated. (**C**) siRNA-transfected McA cells were pulsed radiolabeled with [^{35}S]-Met/Cys for 10 min and chased with Met/Cys complete media for 60 min. ApoB was then immunoprecipitated from cell lysates, incubated with and without Endo H, separated by SDS-PAGE, and visualized with a phosphorimager. (**D**) Cellular apoB100 without Endo H treatment (control, lanes 1–6) was quantified and the relative abundance to control cells was calculated and plotted. (**E**) The intensity of Endo H sensitive (lanes 7–12; lower apoB100 band) and resistant (lanes 7–12; upper apoB100 band) apoB100 was quantified and the ratio was plotted.

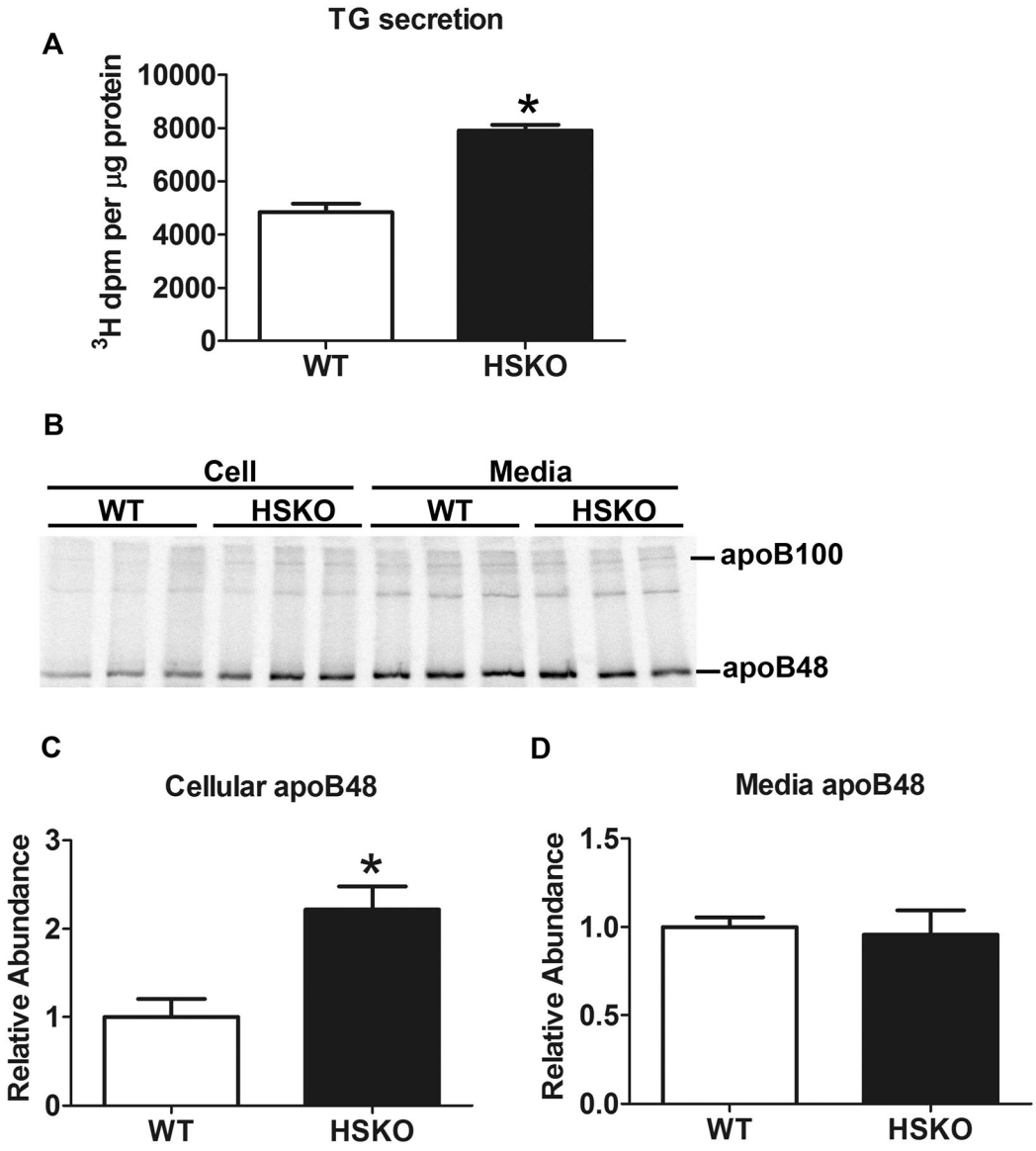

Figure 4. Increased TG secretion and slower apoB trafficking in primary hepatocytes from ABCA1 HSKO mice

(**A**) Primary hepatocytes isolated from WT and ABCA1 HSKO mice were incubated with [^{3}H]-oleic acid in the presence of unlabeled oleate for 6 h. Media [^{3}H]-TG was quantified and normalized to cellular protein content. (**B**) Primary hepatocytes were pulse radiolabeled with [^{35}S]-Met/Cys for 10 min and chased with Met/Cys complete media for 60 min. Both cellular and media apoB were immunoprecipitated, separated by SDS-PAGE, and visualized with a phosphorimager. The band intensities of the cellular (**C**) and media apoB48 (**D**) were quantified and the relative abundance to WT hepatocytes was calculated and plotted.

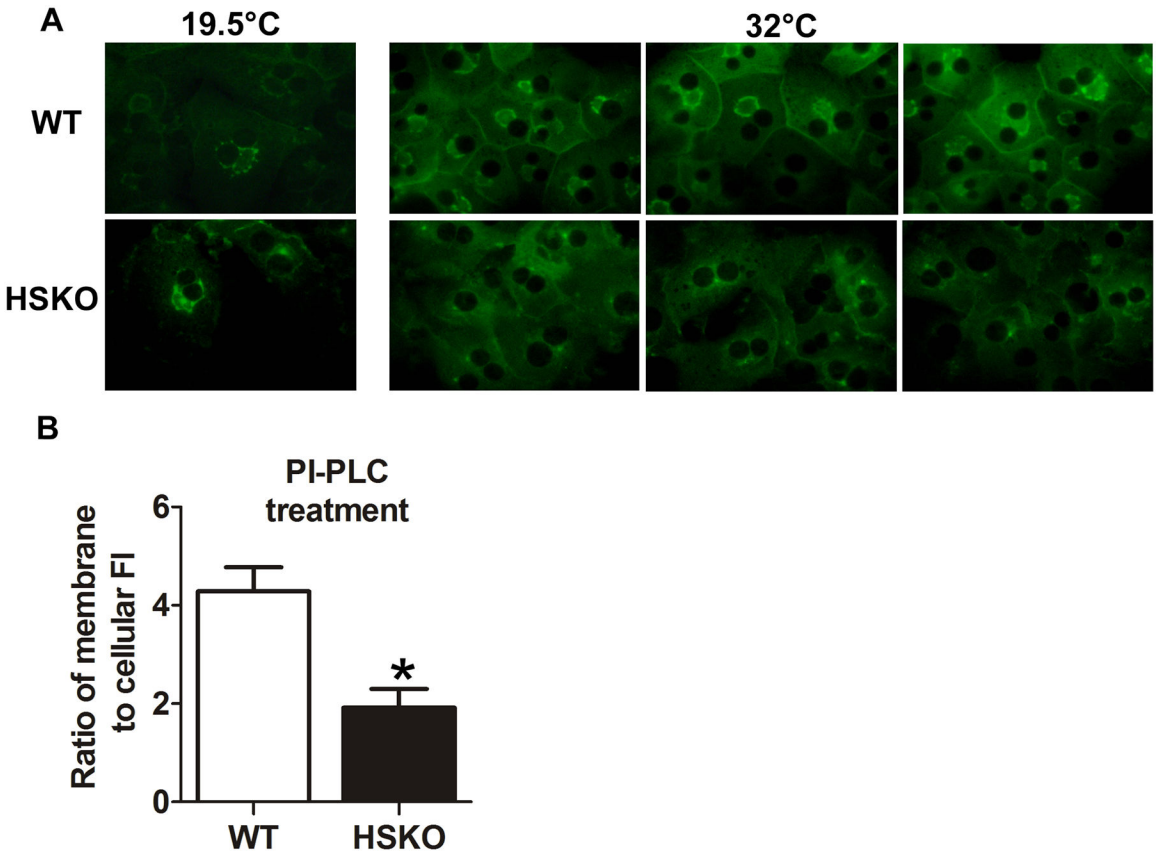

Figure 5. Decreased trafficking of YFP-GPI from the Golgi to plasma membrane in ABCA1 HSKO hepatocytes

(**A**) Primary hepatocytes isolated from WT and ABCA1 HSKO mice were infected with adenovirus expressing YFP-GPI for 24 h. Cells were incubated at 19.5°C for 2 h to accumulate YFP-GPI in the Golgi with cycloheximide added during the last 30 min to prevent further protein synthesis. Cells were warmed to 32°C and incubated for 20 min to release the temperature block, allowing movement of secretory proteins to the plasma membrane. Cells were then fixed and imaged under a florescence microscope. (**B**) At the end of release at 37°C, hepatocytes were treated with PI-PLC at 19.5°C for 2 h before media and cell lysates were collected. Fluorescence intensity (FI) was measured and the ratio of membrane to cellular FI was plotted.

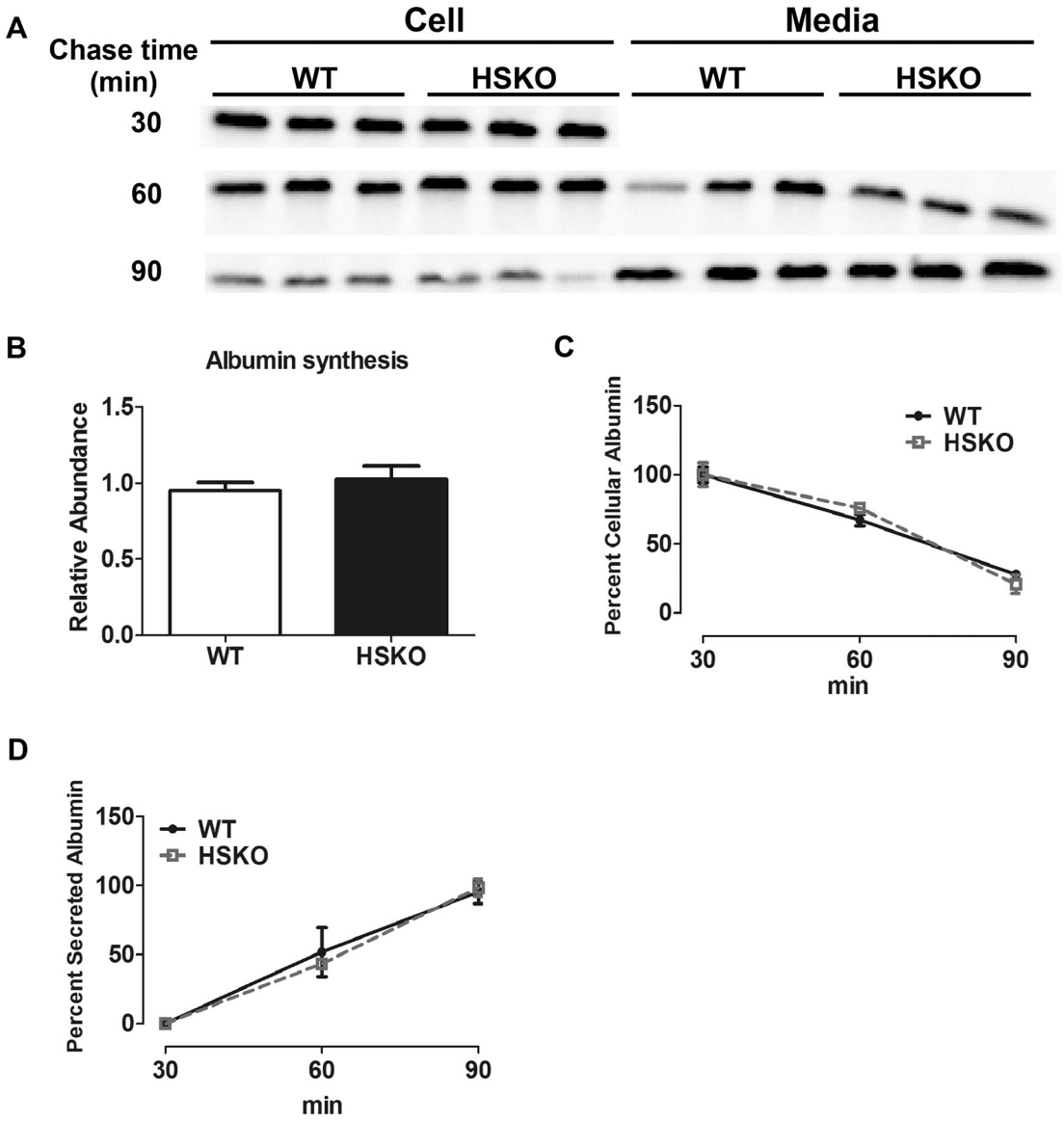

Figure 6. Albumin secretion kinetics was not altered in ABCA1 deficient primary hepatocytes

(**A**) Primary hepatocytes isolated from WT and ABCA1 HSKO mice were radiolabeled with [^{35}S]-Met/Cys for 15 min and chased for 30, 60 and 90 min. Albumin was immunoprecipitated from cell lysates (30, 60 and 90 min chase) and media (60 and 90 min chase), separated by SDS-PAGE, and visualized using a phosphorimager. (**B**) The intensity of albumin bands in panel A was quantified. Thirty-min chase was set as the initial time point and cellular [^{35}S]-albumin abundance was calculated relative to WT. (**C**) The percentage of [^{35}S]-albumin at 30 min chase remaining in cells at each time point was calculated and plotted. (**D**) The percentage of cellular [^{35}S]-albumin at the 30 min chase that was secreted into medium at each time point was plotted.